Dynamic simulation of two sailing boats in match racing

K. Roncin and J.M. Kobus

Laboratory of Fluid Mechanics, Ecole Centrale de Nantes, France

Abstract

This paper describes current progress made towards the realization of a match-racing simulator. The aim of the project is to be able to simulate and to modify typical situations while introducing quantifiable data for strategic and tactical analysis. The fundamental model consists of six fully coupled equations of the dynamics of two boats. The largest possible number of variables is taken into account, even though some are initially approximations. The influences of the three attitude angles on the hydrodynamic forces are taken into account using the 'experiment planning method' applied to towing-tank tests. For the aerodynamics, empirical models (for example IMS) are adopted. The interaction between the two boats is obtained by representing the sail perturbation by means of a single horseshoe vortex and a self-preserved viscous plane wake. The simulator has a modular structure, which allows the progressive improvement of each part as studies and knowledge advance. Comparisons with calculations of three-dimensional flows and with wind tunnel measurements validate the interaction model. The results presented show a satisfactory agreement with the polar velocity diagram available for the studied boat, even if more reliable trials at sea are needed, with measurements of boat behaviour, wind and sea state. Simulations allow us to quantify the relative influence of model coefficients on boat behaviour. Thus it is possible to identify which factors must be improved first. Tacking simulations are used to illustrate this possibility. To conclude, an example of the practical use of the simulator is presented by comparing two tactical scenarios for the final part of the upwind leg.

Keywords: aerodynamic interaction, hydrodynamics, match racing, sailing, simulation

Introduction and problematic

Aims of the project

Especially during the Americas Cup, significant investment has been made in facilitating the general public's understanding of match-racing regattas. GPS and real-time 3D virtual reality software have provided some spectacular tools that enable us to show and replay virtual films of the regattas on the Internet. However, competitors who wish to improve their expertise must go further than simply replaying their moves. They need to investigate numerous solutions and to test tactical and strategic options that are different from those already in use.

Only simulation techniques can perform this complementary function. Some match-racing computer games are available that generally have reasonable graphic qualities and which provide a

Correspondence address:
Laboratory of Fluids Mechanics of Ecole Centrale de Nantes
UMR CNRS 6598
France
Tel: (33) 02 40 37 25 71
Fax: (33) 02 40 37 25 23
E-mail: kostia.roncin@ec-nantes.fr
jean-michel.kobus@ec-nantes.fr

good introduction to tactics and strategy. However, they don't take into account the precise characteristics of boats: the need to maintain the speed of a game limits the amount of real-time calculation that can be done, which necessitates a simplification of the modelling of forces and dynamic behaviour.

Our objectives differ from those of the creators of games. Our ultimate aim is that simulation should become a standard tool for tactical steering optimization and, in addition, be used in boat design.

As the simulator is designed for practical use, the technical objectives are that the simulator benefits from the user-friendliness and graphic qualities of a game, while offering greater accuracy and a set of tools for analysis and optimization.

Finally, although the simulator must be built from an engineering perspective, it also has a scientific utility. On the one hand, it provides a starting point for development and scientific collaboration and it guides research in a practical and useful way. On the other hand, it allows the rapid application and analysis of scientific results. Thus, when the work of a research programme in sailing is centred on a simulator, the simulator becomes the structuring element of the whole programme.

Methodology for the simulator construction

The construction of a sailing simulator is an on-going project involving a succession of steps: the production of models for all the variables, validation of these models, global validation (ideally at each step), improvement of the models, and so on.

The first step is to prove that a simulator is able to perform simulations that are representative of the behaviour of two boats in match racing. We will demonstrate some reliable results for key problems, like steady heading sailing (equivalent to a velocity prediction program (VPP)), tacking and crossings in the tactical problems of close sailing.

To provide useful conclusions, a quantative analysis is needed with a controlled margin of error. Also, the simulator has to be sufficiently sensitive to detect the influence of the parameters on which the optimization would be applied.

Although we should take into account the greatest possible number of variables affecting boat behaviour, we must concentrate on modelling the most important of them. The ideal case is when the different models are equally precise, but this balance is difficult to achieve and to maintain permanently, so large is the field of investigation.

Our fundamental model takes into account two boats with six degrees of freedom of movement. To be consistent, pitch (or trim angle) and heave are taken in account in the modelling of forces.

Because forward speed is the factor that acts most directly and strongly on the stationary hydrodynamic forces, these forces must be included in the model as they are essential for performance prediction. We will also treat aerodynamic interaction as an essential factor for studying tactics in match racing.

In the current version, the simulator works with two one-design 'First-Class 8' boats. The reason is that this boat, 8 m in length, is very popular in France and commonly used for match racing, facilitating the global validation of the simulator results at sea. A model of the boat, at a scale of 1/2.7 has been tested intensively in the towing tank of the Ecole Centrale of Nantes. More than 250 test results are available concerning the six components of hydrodynamic forces as functions of boat attitude, e.g. Roncin (2002). Thus, the hydrodynamic forces on the hull and keel are modelled from these experimental results. It should be noted that the same technique could have been applied with CFD calculations of flows and forces.

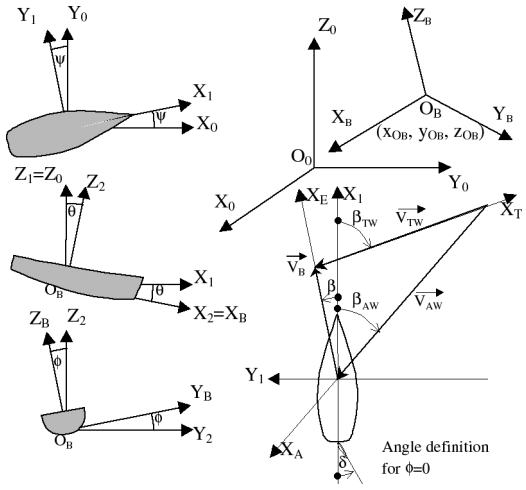

Figure 1 Frames of reference and angle definition

Notations and coordinate systems

Notations and coordinate systems were consistent with the ITTC recommendations (1993).

R_0	Galilean frame of reference related to Earth. The origin is on the free surface, axis X_0 is toward geographic north and Z_0 up to vertical.
R_B	frame of reference of the boat. The origin is at the nominal gravity centre, X_B forward, Y_B to port.
R_A, R_E	co-ordinate systems used for modelling the aerodynamic and hydrodynamic flows respectively. For tactical problems we use also a co-ordinate system in which X_T is the true wind direction. The boat position is known at all times with the attitude and the position vector.
$(\psi, \theta, \phi)^T$	attitude defined by Cardan angles
ϕ	heel angle
θ	pitch (trim) angle
ψ	yaw angle
$\vec{P} = \overrightarrow{O_0 O_b} = (x, y, z)^T$	position vector
$\vec{V}_B$	velocity of the gravity centre in (R_0)
S_{W0}	upright static wetted area surface $(\psi = \theta = \phi = 0)$
L_{WL}	length of the water line
$R_n = V_B L_{WL}/v$	Reynolds number
v	kinematic viscosity of water
g	gravity
$F_n = V_B/\sqrt{L_{WL}.g}$	Froude number
$\vec{V}_{AW}$, $\vec{V}_{TW}$	apparent and true wind velocity
VMG (velocity made good)	$\vec{V}_B . \vec{V}_{TW} / \lvert \vec{V}_{TW} \rvert$
β_{AW}	apparent wind angle between $\vec{V}_{AW}$ and X_1.
β_{TW}	true wind angle between $\vec{V}_{TW}$ and X_1.
β	leeway angle
δ	rudder angle
ρ_W, ρ_A	water and air mass density
h	height of the rig
Δ	boat displacement
$\{A\}$	dynamic tensor
$\{V\}$	kinematic tensor
VPP	velocity prediction program

Simulator structure

The boat is taken as a rigid body. Schematically, the fundamental principle of the dynamic is written in the boat reference frame as follows:

$$\begin{Bmatrix}\text{hydrodynamic}\\ \text{forces}\end{Bmatrix}_{O_B, R_B,} + \begin{Bmatrix}\text{aerodynamic}\\ \text{forces}\end{Bmatrix}_{O_B, R_B}$$

$$+ \begin{Bmatrix}\text{hydrostatic and gravity}\\ \text{forces}\end{Bmatrix}_{O_B, R_B} = \begin{Bmatrix}\text{dynamic}\\ \text{tensor}\end{Bmatrix}_{O_B, R_B}$$

The links between dynamic, kinetics, attitude and boat position are implemented according to the principle shown in Fig. 2.

The simulator was developed using Matlab-Simulink because this environment is particularly suitable for modular conception (Fig. 3). Each element can be modified easily and independently when the understanding and the models of phenomena have been improved.

Modelling of the forces

Hydrodynamic forces

Stationary hydrodynamic forces

Unlike sails and rigs, the hull and its appendages can be considered as a rigid body. This fact simplifies

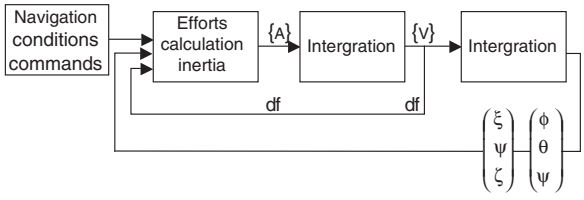

Figure 2 Implementation principle

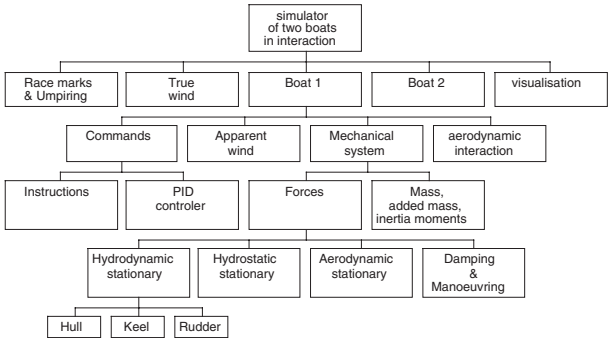

Figure 3 Simulator structure

modelling of the hydrodynamic forces because it depends on fewer working parameters (forward speed, attitude angles and displacement). They vary very little, and generally they affect only speed, so a reduced set of combinations of parameter values can be used to build the model (typically 128 trials). The modelling is facilitated by using the results of trials performed according to the experiment planning method, e.g. Schimmerling (1998) and Roncin (2002). This method can be generalized to obtain models from all types of experimental or calculation results. It is based on response decomposition in an additive form. Any coefficient, C, relative to hydrodynamic forces is assumed to depend on five factors and can be expressed as:

$$C(V_B, \phi, \theta, \beta, \Delta) = \bar{C} + E_1C(V_B) + E_2C(\phi) + \ldots + E_5C(\Delta) + E_{12}C(V_B, \phi,) + E_{13}C(V_B, \phi,) + \ldots + E_{45}C(\beta, \Delta) + E_{123}C(V_B, \phi, \theta) + \ldots + E_{345}C(\theta, \beta, \Delta) + E_{1234}C(V_B, \phi, \theta, \beta) + \ldots + E_{2345}C(\phi, \theta, \beta, \Delta) + E_{12345}C(V_B, \phi, \theta, \beta, \Delta)$$

$\bar{C}$ is the mean of C values over the whole experiment plan.

Each simple effect is a function of a single influence factor, and interactions of order 2, 3, 4 and 5 are respectively functions of all combinations of 2, 3, 4 and 5 factors respectively. This formulation leads to the construction of an order 5 tensor for each hydrodynamic non-dimensional force on the hull and keel. When the weaker effects are neglected, the decomposition gives a simple and quick model that is convenient for real-time calculation. Tools of statistical analysis complete the method, making it possible to check for modelling error.

Only the modelling of hydrodynamic resistance will be presented here. As with towing-tank tests, it is necessary to extrapolate the results at full scale. The classic ITTC 57 method is used. Its principle is to assume that the total resistance, R_T, and the coefficient C_T can be written as:

$$C_T = R_T/0.5 \cdot \rho_W \cdot S_{w0} \cdot V_B^2 = C_W + (1 + k) \cdot C_f$$

Wave resistance coefficient, C_W, depends mainly on Froude number, F_n, and friction coefficient, C_f, depends mainly on Reynolds number, R_n. To respect free surface effects and wave pattern, the towing tank tests are done according to Froude similitude. So, C_W is assumed to be the same for model and boat. We can write:

$$C_{W\,boat} = C_{W\,model} = C_{T\,model} - (1 + k)C_{f\,model}$$

and

$$C_{T\,boat} = C_{W\,model} + (1 + k)\, C_{f\,boat}$$

Thus $C_{T\,boat}$ is obtained by measuring $C_{T\,model}$ and calculating C_f at the Reynolds numbers of model and boat, according to the ITTC 57 formula:

$$C_f = C_{fITTC57} = 0.075/(\log_{10}R_n - 2)^2$$

The form factor, k, depends on the hull shape and it is assumed to be the same for model and boat. A specific experimental procedure, using tests on models at low speeds, e.g. Prohaska (1996), allows estimation of k. Towing-tank tests show that k depends not only on ϕ, e.g. Teeters (1993), but also on β. Thus a model for

$$k = k_0 + \delta k(\phi, \beta)$$

has been built by an identification method. We find:

$$\delta k(\phi, \beta) = k_{|\phi|} \cdot |\phi| + k_{\phi^2} \cdot \phi^2 + k_{\beta^2} \cdot \beta^2 + k_{\beta\phi} \cdot \beta \cdot \phi$$

The coefficients of this model are given in Table 1.

Table 1 Model for the form factor of a First-Class 8

k_0	$k_{\lvert\phi\rvert}$ (rad^{-1})	k_{ϕ^2} (rad^{-2})	k_{β^2} (rad^{-2})	$k_{\beta\phi}$ (rad^{-2})
0.15	–0.19	0.02	1.3	0.35

The modelling of total resistance can be obtained with those of C_W. After applying the response decomposition, the errors made when neglecting each term independently are calculated. Table 2 shows the mean relative error, e, on C_W versus the neglected effect (with constant Δ).

The E_{1234} term represents the error of measurement rather than a true interaction; thus the following terms, which cause a smaller error when they are neglected, cannot be regarded as significant.

Thus, the truncated model can be expressed as follows:

$$C_W = E_1C_W(V) + E_3C_W(\theta) + E_4C_W(\beta) + E_{13}C_W(V,\theta) + E_{23}C_W(\phi,\theta) + E_{14}C_W(V,\beta)$$

This model gives a mean relative error of 2.3% on the complete experimental series of 128 results. We can note that this result shows the significant influence of the trim angle, θ, on hydrodynamic drag because it appears in a simple effect and in two interaction effects with V_B and ϕ. This confirms the necessity to take into account this degree of freedom in the simulator. As an example, Fig. 4 shows the interaction effect $E23C_W(\phi,\theta)$.

Wave action

The model proposed by IMS, e.g. Claughton (1999), was used to estimate wave action as a simple addition of the mean resistance induced by waves. This model

Table 2 Relative error on C_W versus the neglected effects

E…	1	4	13	23	3	14	1234	
Var.	V_B	β	$V_B\theta$	$\phi\theta$	θ	$V_B\beta$	$V_B\phi\theta\beta$	
ε %	46	7.5	3.4	2.6	2	1.9	1.6	
E…	123	124	24	12	2	24	134	234
Var.	$V_B\phi\theta$	$V_B\phi\beta$	$\theta\beta$	$V_B\phi$	ϕ	$\phi\beta$	$V_B\theta\beta$	$\phi\theta\beta$
ε %	1.4	0.8	0.7	0.6	0.6	0.6	0.6	0.4

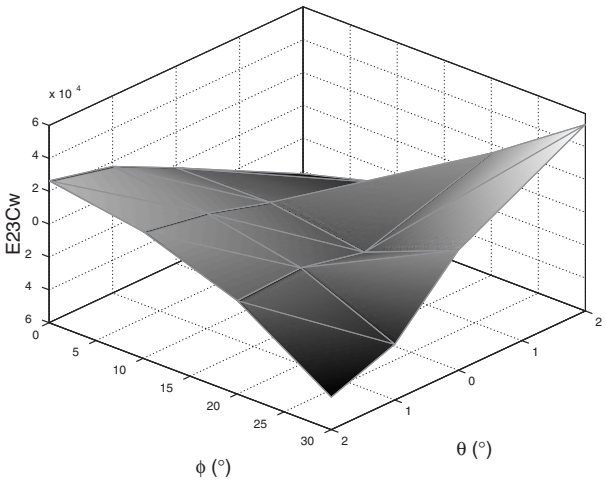

Figure 4 Interaction effect $E_{23}C_W(\phi,\theta)$

is easy to calculate. However, the accuracy is doubtful in following seas because the model has been identified only with head waves calculations. Although this model is convenient for mean performance estimation, it does not satisfactorily represent temporal behaviour in dynamic simulations. Harris (1998) proposes such an approach, based on Froude–Krylov wave forces calculation combined with a strip theory method. This kind of method involves a temporal representation of the sea surface that is not yet implemented in our simulator.

Added inertia and linear damping coefficients

In the current version of the simulator, added inertia and linear damping have been estimated from simple formulae by strip theory on an ellipsoid, e.g. Masuyama (1993) and Keuning (2003). But it is possible to improve these estimations by calculation with panel method codes currently available in the naval hydrodynamics community.

Hydrostatic and gravity efforts

The model for the hydrostatic effort was obtained from measurements of forces and moments at zero speed. It is also easy to compute the hydrostatic efforts; all hull design programs do so.

Manoeuvring efforts

We have not yet found the means of correctly evaluating the manoeuvrability hydrodynamic derivatives according to the angular velocities for the hulls of

modern sailing boats. However, we are helped by the fact that these boats are quite flat. So, the effects of the lifting surfaces (keel, rudder blade and sails) are dominant in gyration compared with the effects on the hull. Most of the effects of the angular velocities on roll and yaw damping are taken into account by considering the forces on the hull and on lifting surfaces (keel and rudder blade) separately. For instance, for estimating the hydrodynamic forces on the keel and rudder, the flow speed is computed respectively at the keel and rudder surface centre. In the same way, we use the calculated velocity at the sail centre of effort for determining the apparent wind speed at each instant. Such calculation of the incident flow on each lifting surface produces automatically a damping of rotation movements. The addition of the effects of sails, keel and rudder blade dampens the rolling and the yawing and strongly affects manoeuvring behaviour.

Thus, having checked that the missing derivatives concerned with the hull had a weak influence on behaviour in operation, for the time being we can be satisfied with a rough estimation of them.

Hydrodynamic interaction

Hydrodynamic interaction between sailing boats is a complex phenomenon that involves the wave pattern, the vortex wake of the keel and the viscous wake of the canoe body and keel. This interaction has been neglected in the current version of the simulator but it could be included if necessary.

Aerodynamic efforts

Choice for sail modelling

At first, a panel method code, e.g. Guilbaud (1997), was used to obtain an estimation of forces on sails. The conclusion of this experiment was that building an aerodynamic force model suitable for simulation requires more than the flow calculation. It is also necessary to determine the choice of settings that produce the best performance for each apparent wind direction, and to distinguish between the permanent settings and those made by the crew during manoeuvre (e.g. boom direction and jib clew). Sail settings and the deformation of rigging and sails complicate the problem. Such studies are lengthy and the results are often inconclusive.

Although the three-dimensional code we used is a powerful tool, the force calculations are limited to some ideal flow cases. So, the work is still complicated by intrinsic limitations of the panel method because of numerical problems with some classic sailing configurations. Continuing in such a way would have unbalanced the general approach to the detriment of the hydrodynamic analysis. Furthermore, as we don't yet have any means to validate the computation with laboratory experimental results or real navigation trials, a self-adjusted empirical model has been chosen for the initial version of the simulator. This model has the advantage of being validated by observations of numerous regattas by IMS, e.g. Claughton (1999).

Aerodynamic interaction

Aerodynamic interaction is one of the main weak points of available simulators. It is nevertheless an essential component of tactics, particularly in match racing. Interaction must therefore be studied with the same care as the aerodynamics.

While a boat is sailing, a nearby opponent's boat disturbs the incident flow intensity and thus the efforts on sails. This interdependency can be represented by a loop system, as shown in Fig. 5.

The disturbance can be considered to be a function of the relative positions of the boats and of the vortex circulation on the sails and in the wake. This circulation directly depends on the lifting force applied on the sails. As a first approach, we adopt a highly schematic but consistent model for aerodynamic interaction. The principle is to represent the

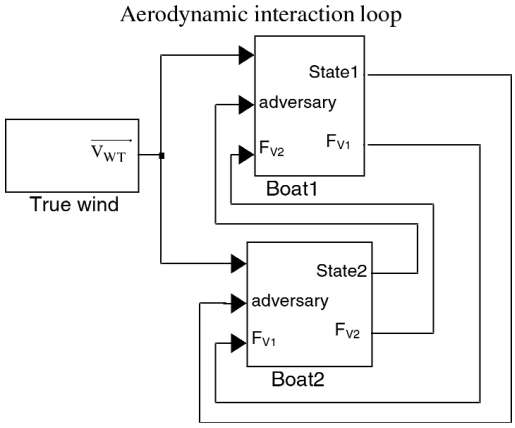

Figure 5 Principle of interaction implementation

opponent's actions as simply as possible and then to adjust the results following comparison with the most complete calculated results available, that is to say, Caponnetto's results (1997). To do that, each of the two boats is figured by a horseshoe-shaped vortex. The vortex intensity, Γ, is obtained from the total lift force on the sails as:

$$\Gamma = -\frac{\text{Lift}}{\boldsymbol{h} \cdot \rho_A \cdot \boldsymbol{V}_{AW}}, \text{ where } \boldsymbol{h} \text{ is the rig height}$$

The measurements carried out in a wind tunnel by F. and V. Nivelleau (1994) show that the most important deflection generated by a sailing boat is located in the wake (Fig. 9(a)). This observation emphasises the pertinence of horseshoe vortices to figure the influence of the sailing boat. This kind of representation is currently the basic method used to model the air flow around sails, whether for the lifting line, e.g. Euerle (1993) and Sugimoto (1999), or for the 'Vortex Lattice Method', e.g. Caponnetto (1997, 1999).

The vertical part of the horseshoe vortex has a height h, corresponding to the overall span. $\vec{V}_{p1}$ and $\vec{V}_{p2}$ are the perturbation of $\boldsymbol{V}_{AW\infty}$, the far-field apparent wind velocity, induced by the vertical bound vortex and by the trailing horizontal vortices respectively. They are calculated in the median plan, $z = 0.5\,h$.

The disturbance velocity field is the field induced by the complete horseshoe vortex. It is added to the incident velocity field to get the final incident velocity. Thus, the apparent wind speed can be calculated in any points (x, y) around the boat as:

$$\vec{V}_{AW} = \vec{V}_{AW\infty} + \vec{V}_{p1} + \vec{V}_{p2}$$

Using the Biot and Savart law for each horseshoe vortex part, the following formulas are found:

$$\vec{V}_{p1} = \kappa \cdot \Gamma \cdot h/(2 \cdot \pi \cdot \sqrt{r^2 + h^2 \cdot r^2}) \Big|_{x_M}^{-y_M}$$

$$\vec{V}_{p2} = \kappa \cdot \Gamma \cdot h/(2 \cdot \pi \cdot (y_M^2 + h^2)) \Big|_{x_M/\sqrt{r^2 + h^2}}^{0} - 1$$

with $x_M = (x - x_{adversary})$, $y_M = (y - y_{adversary})$

and $r^2 = x_M^2 + y_M^2$

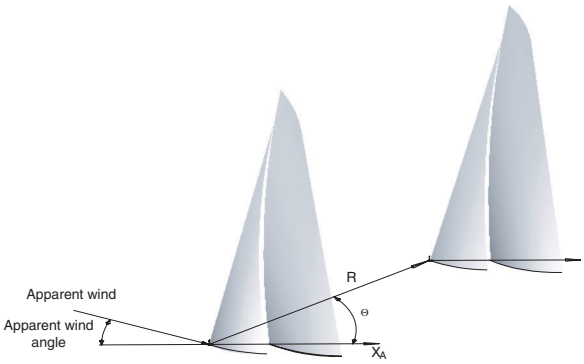

Figure 6 Caponnetto's protocol for interaction

The coordinates are expressed in the aerodynamic frame of reference (R_A), shown in Fig. 6. The κ coefficient is defined to eventually adjust the model according to available results or to measurements. All the results presented have been obtained without setting κ ($\kappa = 1$).

Fig. 7 shows a first comparison with Caponnetto's three-dimensional calculation. The comparison protocol is shown in Fig. 6. The second boat rotates around the key boat with an angle θ_c; the distance between the two boats is 0.5 times the overall span of the rig, h. The vortices are located along the mast of each boat.

It is worth noting that the results shown in Fig. 7 depend not only on the interaction model but also on the method used to compute the efforts on sails. One observes in Fig. 7 that the results are sensitive to the lift coefficient used by Myers or to those of the IMS ones, e.g. Claughton (1999). In order to appreciate the importance of the interaction model, it is easier to compare the very field of flow, i.e. its speeds and local directions.

One can observe in Fig. 7 that with the single horseshoe vortex model, the results are very close to Caponnetto's calculation, especially when using the IMS coefficients. Fig. 7 also shows that the model is consistent when the distance between the boats increases. The calculations shown in Fig. 8 take into account the experimental conditions fixed by F. and V. Nivelleau.

Fig. 7 shows that the calculated deflections are less important than in experiments. Of course, the wake dissipation is not taken into account in this simple model. When the boats are sailing close-hauled, we

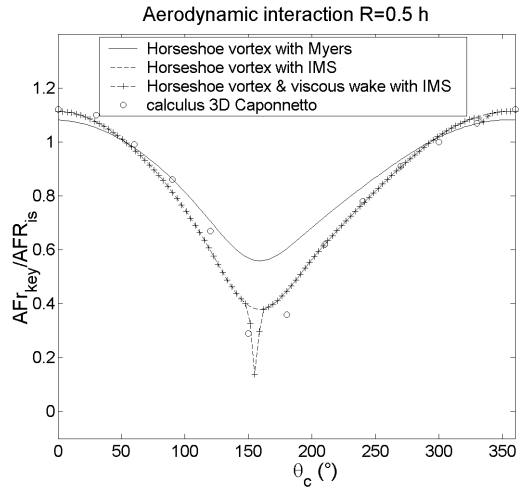

AFr = Fr/0.5ρ_A . $V_{AW\infty}{}^2$,

Fr = propulsive force along boat axis

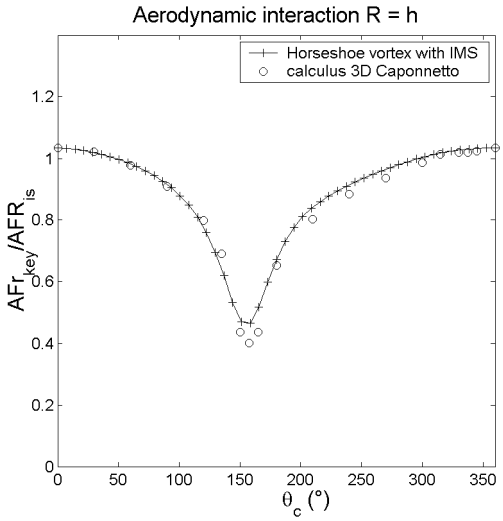

Figure 7 Comparison of single horseshoe vortex model with 3D Caponnetto's calculation

can assume that this dissipation is not significant when considering the characteristic distances between boats during match racing (a few boat lengths).

The tests made by V. and F. Nivelleau show that the wake keeps its effects far from the sailing boat (Figure 9(a)). Thus, we tried to take into account the viscous wake to improve consistency with the experiments of F. and V. Nivelleau (1994).

A model was added to represent this effect and the influence of the Reynolds number on the flow. We used a plane and self-preserved wake to calculate the

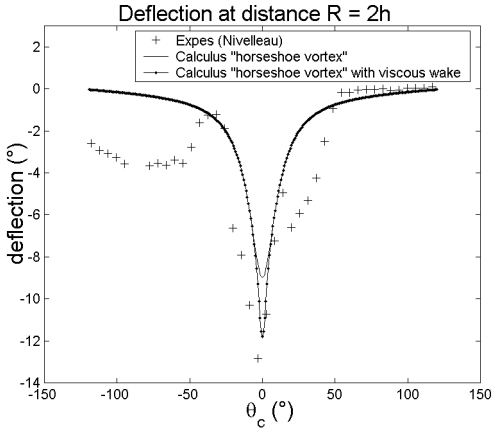

Figure 8 Comparison between model and measurements

viscous effects (Fig. 9(c)). It is possible in this case to relate the velocity disturbance with the drag of the sails. Tennekès (1974) expresses the mean speed default in a plane self-preserved viscous wake as follows:

$$\vec{V}_{p3} = 1.58 \cdot V_{AW\infty} \cdot \sqrt{\Theta / x_M} \cdot e^{\frac{\xi^2}{2}} \cdot \vec{x}_A$$

with $l/\Theta = 0.252 \cdot \sqrt{x_M/\Theta}$ and $\xi = y_M/l$

$\vec{X}_A$: unit vector of X_A axis

l: half width of the wake at $\vec{V}_{p3} = 0.5 \cdot \vec{V}_{p3max}$.

The obstacle is at (0, 0) and (x_M, y_M) is the point where $\vec{V}_{p3}$ is calculated. The momentum thickness Θ is given by:

$$\Theta = D/\rho_A \,.\, V_{AW\infty}{}^2$$

with D = drag/h.

If we substitute Θ in the first two formulae, they become:

$$\vec{V}_{p3} = -1.58 \cdot \sqrt{D/\rho_A \,.\, x_M} \,.\, e^{\frac{\xi^2}{2}} \cdot \vec{x}_A$$

and

$$l = 0.252 \cdot \sqrt{D \cdot x_M/\rho_A} \cdot V_{AW\infty}{}^2$$

Thus the apparent wind velocity in any location of the flow field can be written as follows:

$$\vec{V}_{AW} = \vec{V}_{AW\infty} + \vec{V}_{p1} + \vec{V}_{p2} + \vec{V}_{p3}$$

This very simple model depends on drag, on flow speed and on the relative positions of the two boats.

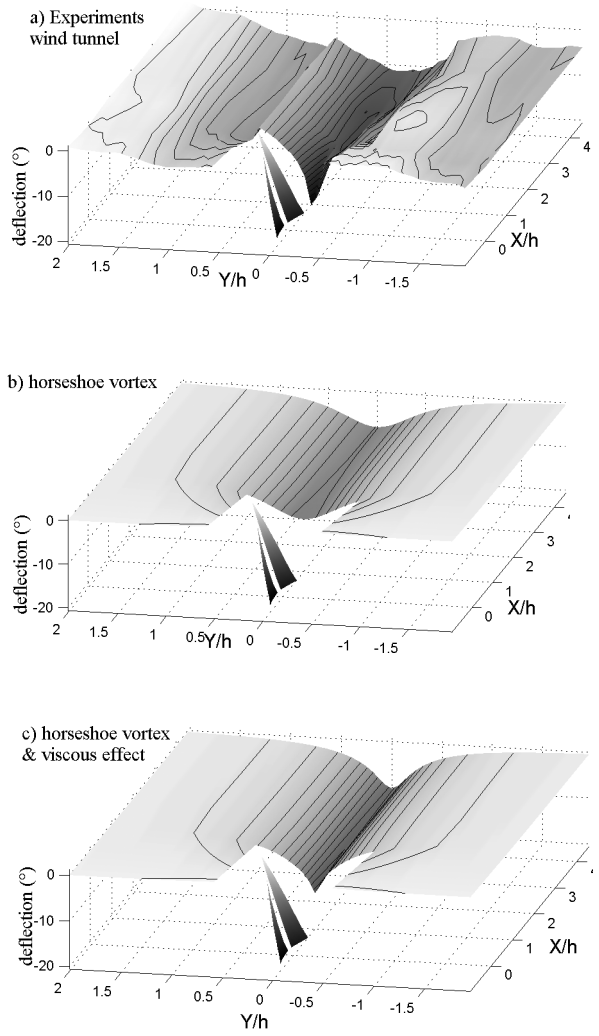

Figure 9 Deflection of streamlines

For comparison, we have put the data of the F. and V. Nivelleau experiment into this model. The lower free vortex of the horseshoe is located at the height of the boom. The z_M altitude of the measured point is given in Table 3, related to the median plan of the horseshoe vortex. It is defined to match the altitude of the measurement probe. The calculation is sensitive to this data. A gap between our calculation and the measurements is probably due to the difference between the intensity of boom whirl and of masthead whirl. A triangular distribution of circulation and a more accurate modelling of the trailing vortices in the wake, which better matches the sails, would probably give better results for this comparison.

Table 3 Data to compare to Nivelleau's experiment

β_{AW} °	V_{AW} m/s	Lift N	Drag N	z_M m	H m
20	16	129.6	29.6	-0.24	1.42

In Fig. 10, the vortex model, which is a function of lift, and the viscous model, which is a function of drag, are superimposed. Upwind, the lift is dominating and the vortex model is the more significant. Downwind, the viscous model becomes more important because drag is increasing and lift is decreasing.

The similarity between the very simplified calculus with the horseshoe single vortex (without settings) and the three-dimensional calculus with Caponnetto's vortex lattice method was rather surprising. Our aim was to test a rough model for exploration, and we are not claiming that this model is a panacea. These

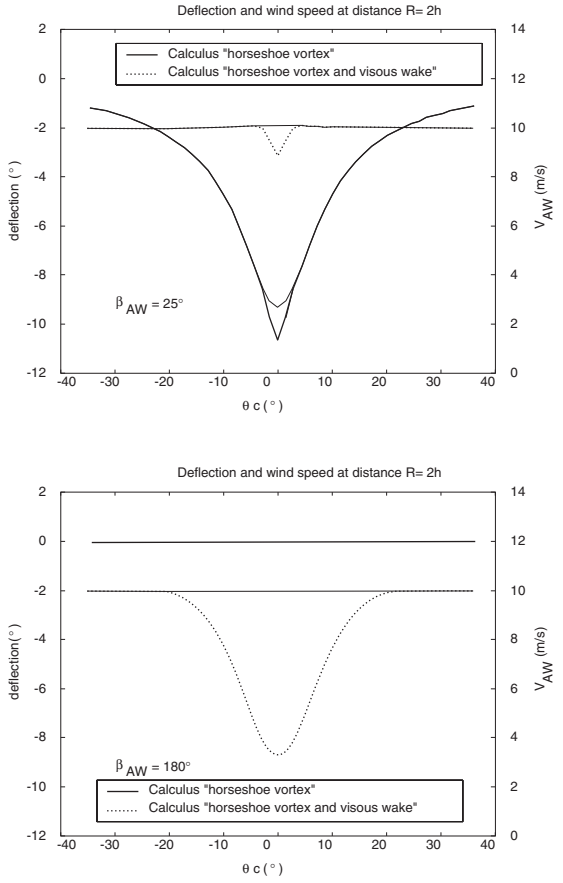

Figure 10 The influences of lift effects and viscous effects in the wake at and β_{AW} = 25° and β_{AW} = 180°

results do not constitute proof of the model's accuracy, but provide an encouraging indication that modelling the aerodynamic interaction with a simple representation is possible and useful for the purposes of simulation.

Examples of results

The following examples have two goals. The first is to illustrate the simulator's potential and to check if its behaviour is relevant for simple navigation cases. The second is to look at the real influence of coefficients that we have roughly determined.

There are two methods for piloting the simulator. The first is to act on the rudder, as on the real boat. In this case, the ability to maintain a heading, or an angle with the wind direction, depends on the operator. This option is already possible, and it will be interesting to see the results when the simulator is run independently by two competitors to simulate a regatta in real time.

For the time being, we prefer to replace the skipper with a PID controller. Certainly, the behaviour of the boat depends on the PID coefficient setting. Even if the PID pilot is not a good helmsman, at least we can be sure that it always reacts in the same way.

Polar diagram and VPP

Here we show the results by means of a polar diagram of boat speed, which classically shows the boat performances. The polar angle is taken between the actual course of the boat and the true wind direction, that is to say $\beta_{TW} + \beta$.

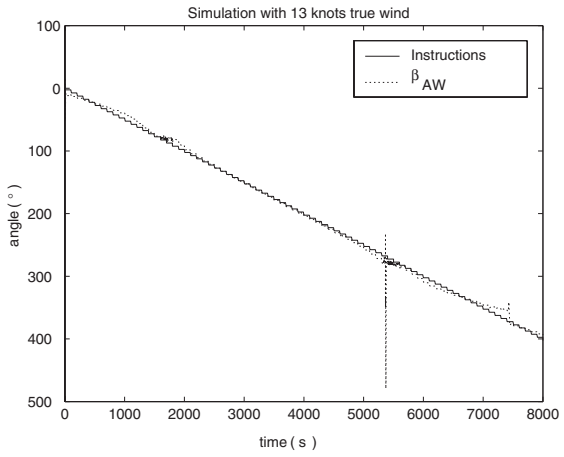

Figure 11 Instructions for polar diagram

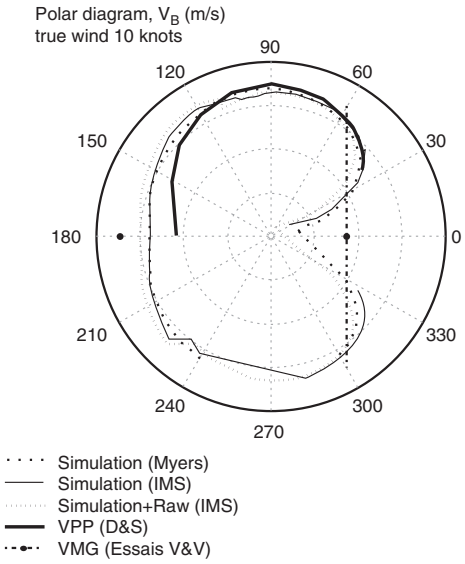

Figure 12 Polar performance diagrams

Because we are using a dynamic simulator, the points on the polar diagram are a succession of converged steady states. The polar diagram is obtained by giving the pilot a succession of constant instructions for $\beta_{AW,}$ like the steps of a staircase. At the end of each step, we consider that the boat has a stationary movement. A little more than 360 degrees rotation is completed within a simulation time of 8000 s. Some instabilities appear in the simulation at two particular points. The first occurs at tacking (β_{AW}#0 and –360°). The other occurs at the setting and the hauling down of the spinnaker (β_{AW}#–80 and –280°) because we are not careful with spinnaker-to-jib exchange. In the present case, the boat is broaching at t = 5400 s.

The polar diagram is plotted with different aerodynamic models (Myers and IMS) and with the IMS model for added resistance in waves (R_{AW}).

We compare our results to those of a commercial VPP (Design System and Services – G.S. Hazen) and to tests published *Voiles & Voiliers* magazine, e.g. Gourmelen (1998). Such tests have no scientific aim and the data for testing their accuracy are not available. This comparison is shown for information because we have no comparable scientific data.

However, this comparison shows that our simulations deviate from tests as the wind increases. These deviations are perhaps a consequence of the sea conditions, that have been rather simplified in our

simulation. Close to the wind, the boat slows down because of wave effects. However, downwind, the boat is pushed by the waves. The wave effect is probably underestimated on the downwind course. This result also underlines the need for scientific tests in real sailing conditions, where all the physical data that affect the boat's behaviour would be measured. On the other hand, we observe that polar diagrams obtained with two different sail models (Myers, 1975 and IMS) are close, e.g. Claughton (1999). This is all the more remarkable since the wind force is higher and the boat reaches its maximum speed.

Tacking

Conditions and simulation results

To simulate tacking manoeuvres, we need to estimate forces on sails with a head wind, but the Myers model, which we used to obtain these forces, does not provide results below 15 degrees of incidence. As a first approximation, we consider that the lift is varying linearly between 0 and 15 degrees for the main sail and between 6.8 and 15 degrees for the jib (values obtained from three-dimensional calculus with a panel method code and IMS). The jib lift is taken at zero between 0 and 6.8 degrees. This model, which may be optimistic, could be improved when the simulator results are compared with real navigation tests.

The presented simulation has been made with a Runge–Kutta algorithm of order four and a time step of 0.2 s.

The true wind speed is 5m/s (approximately 10 knots). The PID pilot controls the rudder angle for obtaining a predefined apparent wind angle β_{AW}. The simulation can also be done with a specified function $\delta(t)$, but a difficulty arises from the fact that, before tacking, and during the last part of tacking, helmsmen are steering according to the wind.

Tacking starts at t = 200 s and the data are shown between 195 s and 250 s (Fig. 13).

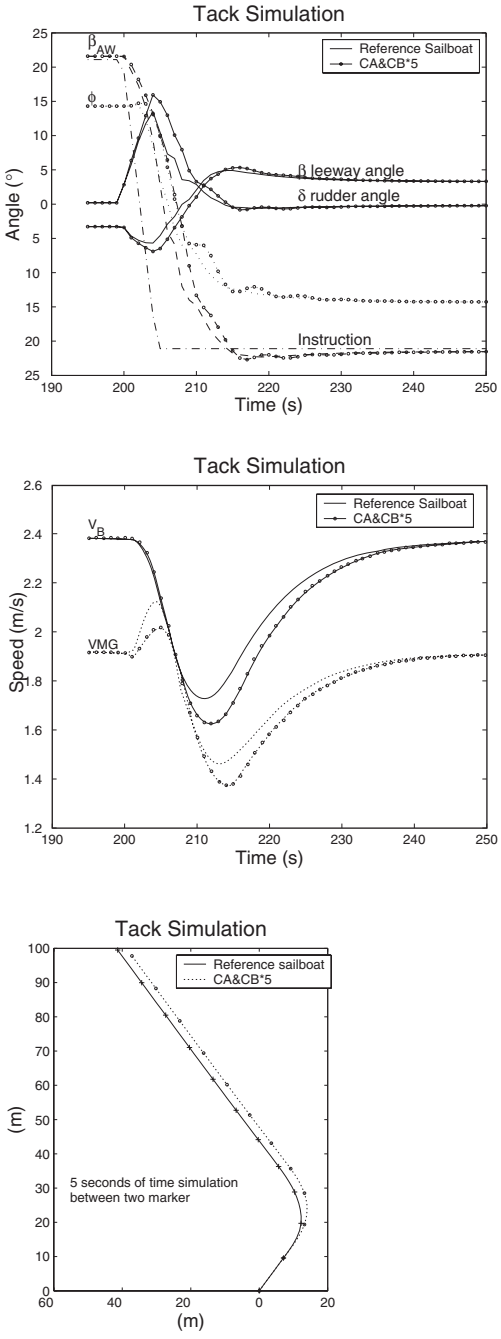

Figure 13 Tack simulation and influence of hydrodynamic inertia and damping in rotation

Influence of hydrodynamic coefficients on tacking

The simulation can help us to quantify the influence of the coefficients used in the models on the global behaviour of a boat. Tacking was chosen to illustrate this.

The stationary hydrodynamic model issued from towing-tank tests gives a stationary damping for surge and for sway. These are used in the simulation with the assumption that stationary damping is valid for

dynamic behaviour. We therefore have to be careful not to add coefficients for these moves. The only damping that is not given by the hydrodynamic model issued from basin tests is that along the vertical axis Z_0 in (R_0) and for rotating moves (roll, pitch and yaw). Fig. 13 shows the influence of coefficients that we have roughly estimated, that is to say, hydrodynamic derivatives for hull manoeuvring forces dependent on acceleration and angular velocity.

For the reference boat, the coefficients have been computed by a succinct strip method. For the second boat a very unlikely factor 5 is applied to the coefficients for obtaining observable differences.

Logically, the reference boat reacts faster and the rudder angle necessary to follow the instruction β_{AW} is weaker. Fig. 13(b) shows that the reference boat maintains a higher speed through tacking. After the manoeuvre is completed, its position is superior by 1.5 m to the other boat in the X_T direction of the wind coordinate system (Fig. 1), and 2.5 m in the Y_T direction (Fig. 13(c)).

The weak difference between simulations, regardless of the multiplier factor magnitude, can be explained because, as soon as the boat picks up speed, damping due to lift effects on the sails, keel and rudder becomes important. We show here that this remains true during the transition phase, when the movement is no more stationary than during tacking.

Nevertheless, when the simulator reaches a higher degree of accuracy, correct calculations of rotation added inertia and damping would be of great interest for boat design.

The upwind mark approach

Here two tactical scenarios of the upwind mark approach are compared. Tacticians often discuss this case, which is the subject of many papers, e.g. Richard (2001) and Dumard (2002).

At the beginning of the two scenarios both boats are close to the wind and the first boat is starting (dark trajectory) a boat length ahead of the second.

In Fig. 14, the classic approach, also known as 'wise', is shown in the upper diagram; both boats wait to reach the lay line before tacking. In the lower diagram, the approach proposed by M. Richard and C. Dumard is shown; the second boat (light trajectory)

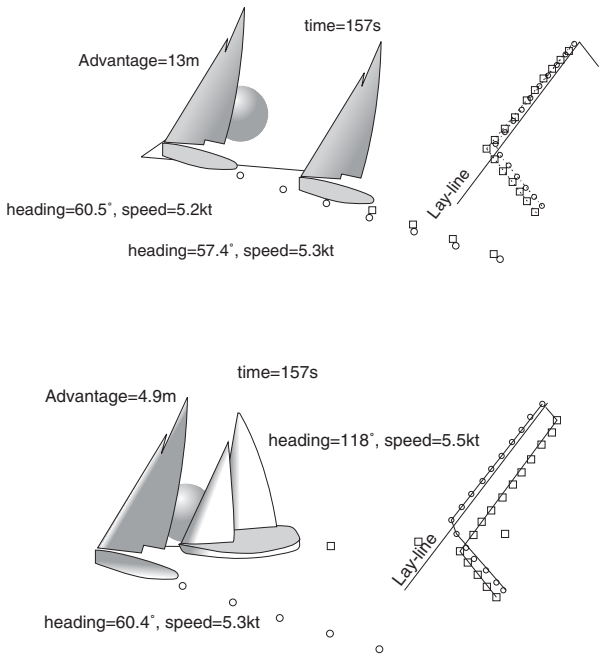

Figure 14 Final views of the animation of two upwind legs at mark approach.

chooses to tack some lengths before the lay line. It will have to tack once more to reach the buoy and this manoeuvre results in loss of time. In fact, in the classic approach the second boat is highly disadvantaged. On the last tack, which leads to the buoy, it is losing more and more distance. The trajectories are convergent. At the beginning of the tack it loses less than 1° in direction and at the end it loses more than 3°. With the second solution the second boat takes advantage of aerodynamic interaction, particularly during crossings, and it gets a more favourable wind.

Finally, the second boat, when choosing the second option, wins a boat length against its adversary on a tack of 1′ 30″. It is slightly behind its adversary but it reaches the buoy having the right of way.

Conclusion and prospects

Our simulator is still being developed and many parts remain to be improved. Nevertheless, the setting up of the equations of the dynamics of a boat was carried out thoroughly, and the principal physical phenomena that influence their behaviour were taken into account.

The simulator offers an efficient means of evaluating the influence of parameter values on the global behaviour of a boat. It is sufficient simply to measure the effects of a variation in each relevant parameter. During the building phase of the simulator, this characteristic makes it possible to improve various models that have initially been treated roughly. The simulator thus helps with planning. In the exploitation phase, this function will be used for the optimization of boats and of their steering.

Even if some phenomena are modelled in a rough way, the first results are in agreement with the observations of sailors. However, when the skipper decides voluntarily to degrade the performance of his boat for tactical reasons (dial up, for example), some models may be temporarily out of their validity domain. Such situations also occur when the boat broaches or falls off and so reaches great heeling and leeway angles. Currently, in order to continue with the simulation, the field of validity of the models is widened by arbitrary means. Some improvements must be made in order to model these extreme situations met during simulation.

With the simulation of boat behaviour and its polar diagram, there is an observable difference between the simulation and the available experiments when the wind increases. This fact is probably due to the effect of sea state but this is difficult to prove because the sea state during the experiments is rarely indicated.

With tacking, the simulation does not currently take into account the gravitational and dynamic forces and moments induced by crew displacement during manoeuvres. The difficulty here does not lie in modelling the forces, but in characterising the scenarios of crew displacements.

In the example provided of the upwind mark approach, simulations applying the simplified model of aerodynamic interaction confirm the observations of skippers, although hydrodynamic interaction is not taken into account because it is regarded as negligible in comparison with the current precision of simulations.

With hydrodynamics, we have benefited from extensive data obtained from towing-tank tests for the first version of the simulator, but such tests are very long and expensive to carry out. The principal prospect will be the use of CFD codes instead of the results of towing-tank tests. Thus, we will be able to build models for other boats by using the same experimental planning method but applied to numerical results.

A similar approach will be adopted for manoeuvrability problems. The results of CFD codes will enable us to identify the manoeuvrability derivatives.

The absolute priority is to undertake tests of validation in navigation. Unfortunately, these measurements are currently missing or incomplete. However, they are absolutely necessary to validate the results of simulations and the pertinence of the models.

References

Caponnetto, M. (1997) The aerodynamic interference between two boats sailing close-hauled. *International Ship Build Progress*, **44**, (439), 241–256.

Caponnetto, M. *et al*. (1999) *Sailing yacht design using advanced numerical flow techniques*. 14th Chesapeake Sailing Yacht Symposium (CSYS), Annapolis, Maryland, 30 January , pp. 97–104.

Claughton, A. (1999) *Developments in the IMS VPP Formulations*. 14th Chesapeake Sailing Yacht Symposium (CSYS), Annapolis, Maryland, 30 January, 1–20.

Dumard, C. (2002) Le près, les petits coups qui rapportent. *Cahier des régates*, Janvier **62**, pp. 14–18. (in French)

Euerle, S.E. & Greeley, D.S. (1993) *Toward a rational upwind sailing force model for VPPs*. 11th Chesapeake Sailing Yacht Symposium (CSYS), Annapolis, Maryland, January, 75–86.

Gourmelen, J.L. *et al*. (1998). Six monotypes à sensation. *Voiles & Voiliers*, Janvier, **323**, 38–50. (in French)

Guilbaud, M. & Rajaona, D.R. (1997) Numerical study of sail aerodynamics. *Transaction of the ASME*, **119**, December.

Harris, D. (1998) *Downwind performance of yachts in waves*. AMECRC, Perth node, Curtin University of Technology Western Australia. http://www.curtin.edu.au/curtin/centre/amecrc/papers/ame98/dharris.html.

Keuning, J.A., Vermeulen, K.J. (2003) T*he yaw balance of sailing yachts upright and heeled*. 16th Chesapeake Sailing Yacht Symposium (CSYS), Annapolis, Maryland, March, 1–18.

Masuyama Yukata (1993) *Dynamic performance of sailing cruiser by full-scale sea test*. 11th Chesapeake Sailing Yacht Symposium CSYS, Annapolis, Maryland, January, 161–180.

Myers, H.A. (1975) Theory of sailing applied to ocean racing yachts. *Marine Technology*, **12** (3), July, 223–242.

Nivelleau, V. & F. (1994) Sillage aérodynamique du voilier – Cartographie générale du sillage – Etude locale (girouette) – interaction de deux voiliers. St Cyr l'Ecole, August–September (in French).

Prohaska, C.W. (1966) *A simple method for the evaluation of the form factor and the low speed wave resistance*. 11th ITTC.

Richard, M. (2001) L'approche de la bouée au vent. *Cahier des régates*, May, **53**, 14–18 (in French).

Roncin, K. (2001) Simulation du comportement dynamique du voilier. *8ème Journées de l'Hydrodynamique*, Nantes, 5–7 March, 325–340 (in French).

Roncin, K. (2002) *Simulation dynamique de la navigation de deux voiliers en interaction*. PhD Thesis, Laboratory of Fluids Mechanic, Ecole Centrale de Nantes (in French).

Talotte, C. (1994) *Adaptation de procédures expérimentales au cas des voiliers en gîte et dérive, comparaison des résultats expérimentaux et numériques*. PhD Thesis, Laboratory of Fluids Mechanic, Ecole Centrale de Nantes (in French).

Teeters, J.R. (Sparkman & Stephens Inc.) (1993) *Refinements in the techniques of tank testing sailing yachts and the processing of test data*. 11th Chesapeake Sailing Yacht Symposium (CSYS), Annapolis, Maryland, 29–30 January, 13–34.

Tennekès, H. & Lumley, J.L. (1974) *A First Course in Turbulence*. The MIT Press, Cambridge, MA, London, England, p 116.

Schimmerling, P. (1998) *Pratique des plans d'expérience*. Edition Lavoisier (in French).

Sugitomo, T. (1999) A method for optimising sail design. *Sports Engineering* **2**, 35–48.